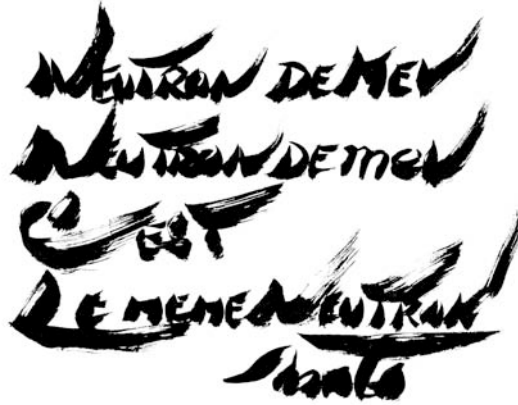


Neutron Production, Moderation, and Characterization of Sources

J. M. Carpenter



NEUTRON DE MEV
NEUTRON DE MEV
C'EST
LE MEME NEUTRON

*Thermalization, Haiku and calligraphy
by Motoharu Kimura (~ 1992)*

Introduction

This essay describes the processes of fission and spallation, which are the means for producing neutrons for most neutron scattering applications. It also describes the moderator arrangements of steady and pulsed sources, cold- and hot-neutron sources and analytical and experimental means for characterizing neutron beams.

1.Primary Source

Two fundamental mechanisms provide neutrons for slow-neutron scattering purposes in present-day research facilities: fission (in research reactors) and spallation (in accelerator-driven spallation neutron sources).

Fission

In reactors, fission takes place when a fissile nucleus (always ^{235}U or ^{239}Pu in practice, although there are a few others) captures a neutron, the nucleus splits into two nearly equal-mass fragments (in large variety) that together carry about 160. MeV of kinetic energy. On average, the process also promptly ($\sim 10^{-15}$ sec) produces about 2.5 neutrons for each fission. Fission

neutrons actually “evaporate” from the initially highly excited fragments and have average energies of about 2. MeV. Each fission event produces a total of approximately 190. MeV of energy: fission fragment and neutron kinetic energy, beta radiation (mostly e^- because fission fragments usually have too many neutrons), and photons (γ rays), all of which appears as heat in the reactor fuel and surroundings, and neutrino energy, which escapes. A small fraction ($\sim 0.5\%$) of neutrons appear after a few seconds delay time. The delayed neutrons are essential for reactor control. One neutron of the 2.5 goes on to cause another fission, usually (after a few microseconds) slowing down to energies at which the fission cross-section is large. Capture in control rods and parasitic processes absorb about 0.5 neutron per fission. This leaves about 1 neutron per fission useable for external purposes.

In round numbers, fission reactors require dissipating about 200. MeV of heat energy for each useful neutron produced. Most (but not all) reactors used for slow-neutron scattering research operate in a steady mode.

The spectrum of prompt fission neutrons as they are born in fission events is the result of evaporation from an originally excited nucleus. The distribution reflects the distribution of neutron energies in the nucleus. Figure 1 illustrates spectrum of prompt fission neutrons in the laboratory coordinate system.[1] Delayed neutrons come from decay of specific excited states of certain specific nuclei, which are rare. As a consequence, delayed fission neutrons are monoenergetic and have energies of a few hundred kilovolts. The delay results from the slow process of beta decay of *precursor* nuclei among the fission fragments, which decays feed the neutron-emitting state.

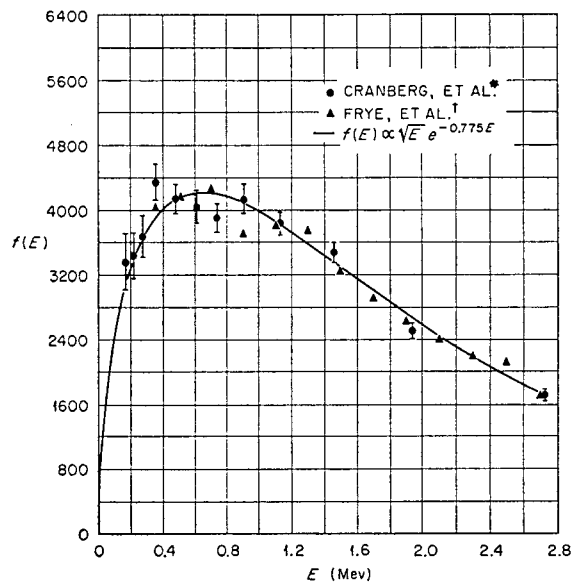


Figure 1. The energy distribution of prompt fission neutrons.[1]

The function shown in the inset has a mean energy of 1.98 MeV. A somewhat more accurate form is $f(E) = \exp(-1.036E) \sinh \sqrt{(2.29E)}$, where E is in MeV. Neutrons emerging from a reactor core have, mostly, collided several times before emerging. The spectrum of emerging neutrons therefore contains lower-energy neutrons and fewer higher-energy ones than in the figure.

Spallation

The term *spallation* refers to a complex of reactions initiated by interaction of high-energy (\sim GeV) particles (p, n, π, \dots) with (typically, in our context) heavy nuclei. W. H. Sullivan and G. T. Seaborg [2] coined the term in April, 1947 to describe the phenomenon, whereby the target emits a fairly large number of neutrons in a multiple-collision process, which was already quite well known. Robert Serber qualitatively described the process in a brief 1947 paper [3]. Enrico Fermi summarized important then-current information in his 1949 lectures [4]. All this goes back to Victor Weisskopf's description of nuclear evaporation processes [5].

In accelerator-driven spallation sources, high-energy particles (invariably protons of ~ 1 GeV energy) from the accelerator impinge on a thick target of dense, high-mass-number materials, e.g., uranium, tungsten, tantalum, or mercury. Here they collide, leaving highly excited nuclei. Neutrons, protons, and pions that emerge from collisions with sufficient energy proceed to collide again and leave further excited nuclei. The excited nuclei shed their energy by promptly evaporating particles (by far, predominantly neutrons) until there is too little left for that process. Then they decay by giving off beta particles (mostly e^+ because the residual nuclei usually have too many protons) and gamma radiation. In practical circumstances, the spallation process produces around 20 neutrons, on the average, for each proton. Most of the neutrons produced emerge from the target, and most are evaporation neutrons with average energies of about 2.0 MeV. A small fraction of the neutrons (a few percent of the total) emerge directly from billiard-ball-like collisions of particles within the nuclei and have energies (hundreds of MeV) distributed continuously up to the incident proton energy. About 60% of the proton beam energy appears as heat in the target; the remainder is mostly neutron separation and kinetic energy. Thus most of the neutrons from spallation sources are like those from reactors, but the small fraction of high-energy, direct-collision neutrons require much more massive shielding than is typical in reactors.

Some installations have used ^{238}U as target material, in which, with a significant probability, excited nuclei may fission instead of or in addition to evaporating particles directly. Then, fission fragments, similar to those produced by slow-neutron-induced fissions, evaporate neutrons. This results in a considerably larger total number of neutrons, at the expense of a larger amount of deposited energy and a small component of delayed neutrons that is undesirable (but tolerable) in pulsed sources.

In round numbers, spallation sources require dissipating only about 30 MeV of heat per useful neutron produced. Most (but not all) research spallation neutron sources operate in a pulsed

mode, with short primary neutron pulses (less than 1 microsecond) and frequencies between 10 and 60 Hz.

Figure 2 illustrates the spallation process.

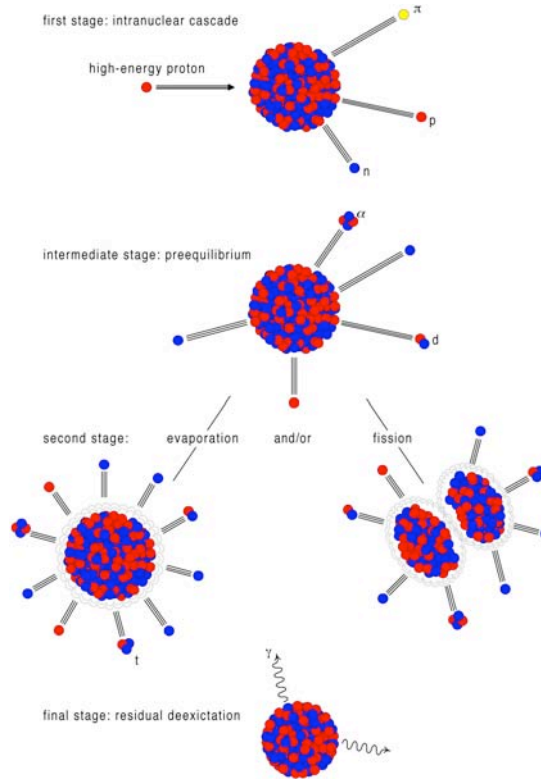


Figure 2. The spallation/fission process. Courtesy L. Waters, Los Alamos National Laboratory.

Spallation Neutron Yields

The yield (that is, the number of neutrons produced per incident particle) of neutrons from spallation reactions varies strongly with the particle energy and the mass number of the target nuclei. In the mid-1960s, John Fraser and his colleagues carried out systematic measurements of the thick-target neutron yields. [6] Figure 3 shows the results.

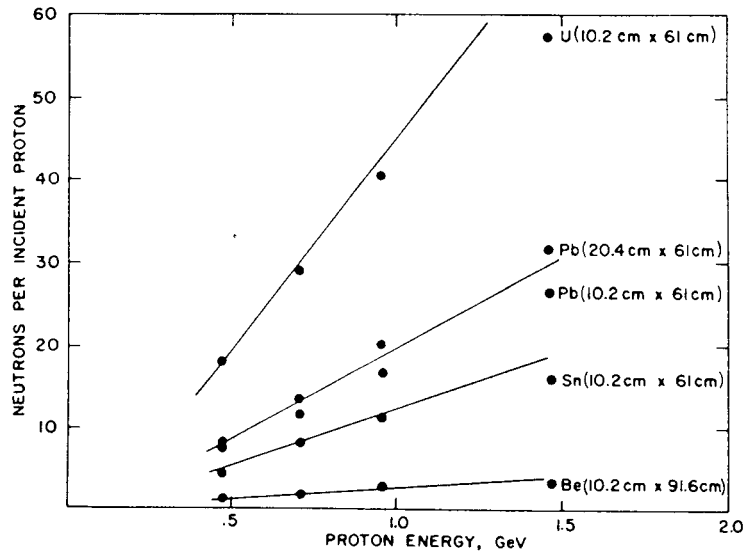


Figure 3. Thick-target yields of neutrons as a function of incident proton energy and target material.[6]

A function that reasonably well correlates the Fraser data is

$$Y(E, A) = \begin{cases} 0.1(E_{GeV} - 0.120)(A + 20), & \text{except fissionable materials;} \\ 50.(E_{GeV} - 0.120), & {}^{238}\text{U}. \end{cases}$$

The yield is approximately a linear function of the mass number, A , of the target material. Up to 1. GeV or so, the neutron yield is approximately a linear function of the energy, with an apparent threshold of 0.12 GeV. A yield proportional to proton energy implies constant neutron production rate per unit of time-average proton beam power. For example, 1-GeV protons on a thick target of tungsten produce about 18 neutrons per proton, about 1 neutron per 56 MeV of proton energy. Accounting for separation energy and kinetic energy of the neutrons and others losses in the energy balance, about 60% of the proton beam energy appears as heat in the target, about 33 meV per neutron in this example. For higher energies, the yield falls off from the linear relationship because of the production and non-productive decay of π^0 particles into pairs of 70-MeV photons. On this account, above 1. GeV the yield goes approximately as $(E_{GeV}/1.0 \text{ GeV})^{0.8}$. [7]

The spectrum of neutrons from a spallation target exhibits a predominant evaporation spectrum of similar form to that of prompt fission neutrons, with a strongly angle-dependent component of direct-collision neutrons extending up to the incident proton energy. Neutrons emerging from a practical target have collided several times, so the distribution is degraded in energy from the as-born distribution. Figure 4 shows the distribution of neutrons as a function of energy emerging from a target of tantalum irradiated by 1-GeV protons, for different angles of emergence. [8]

Just below 1 MeV is the more-or-less isotropic evaporation peak, degraded by collisions in the target. Above about 10 MeV, direct-collision neutrons dominate the distribution, especially in the forward directions. In principle, there should be no high-energy neutrons at angles greater than 90°, but multiple scattering events both degrade and direct backwards some of the high-energy ones initially going in forward directions.

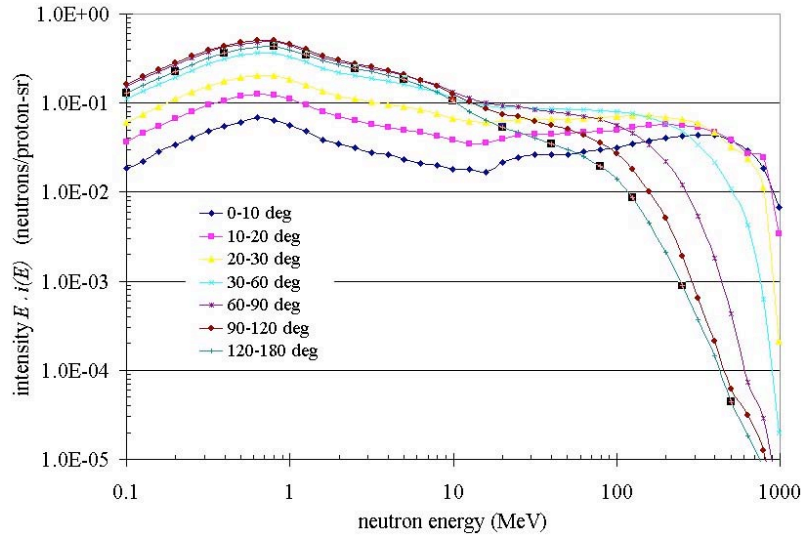


Figure 4. The energy and angular distribution of neutrons emerging from a tantalum target irradiated by 1-GeV protons. The target is 31 cm long, 7 cm wide and 20 cm high. Courtesy B. J. Micklich.

2. Moderators and Moderation of Fast Neutrons

In any case, steady or pulsed, reactor or accelerator, the primary reactions produce most of their neutrons at energies of a few MeV. This is far too high an energy to be useful for slow-neutron scattering, the purposes that we discuss here. Therefore in slow-neutron scattering facilities there are *moderators* arranged around the primary source to slow down the source neutrons to useful energies. In steady sources, the primary moderator is usually a large ($\sim 1 \text{ m}^3$) volume of material—beryllium metal or heavy water, D_2O —surrounding the source. In reactors, the external moderator also serves as a reflector to give neutrons that leak out a second chance to cause a fission therefore to reduce the amount of fuel required to maintain a steady (*critical*) reaction. Meanwhile, neutrons collide with moderator atoms, in each collision losing a fraction of their energy—about 50% in H_2O , about 40% in D_2O , approximately 19% in Be—finally slowing down and coming into thermodynamic equilibrium with the moderating material.[9]

This requires about 16 collisions in H_2O , 29 collisions in D_2O , and 69 collisions in Be.[10] Then, as *thermal neutrons*, they diffuse around until they either leak out into the surroundings or disappear when captured in the material. The best moderator-reflector materials for steady sources are light nuclei (H, D, Be, sometimes C), which slow down neutrons most effectively. But such materials must also have low cross sections for capturing neutrons so that they live long in the reflector and accumulate to high densities; moreover, they must have only modest stopping power for primary source neutrons so that the neutrons slow down in a large volume. These last requirements rule out hydrogenous moderators for use in high-flux research reactors. Figure 5 schematically illustrates the arrangements in a research reactor. Present-day facilities have about 20 beams serving neutron scattering instruments.

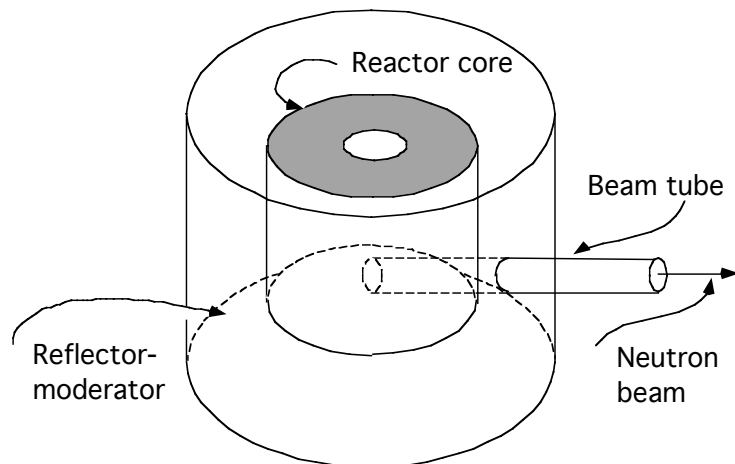


Figure 5. Schematic illustration of a research reactor core and moderator-reflector, showing one beam tube (of many) and an emerging neutron beam.

Figure 6 illustrates the processes that go on in the core and reflector of a research reactor. In the core, fast neutrons from fission travel from collision to collision, losing energy until they cause another fission or leave to enter the reflector. In the reflector, neutrons collide again and again until they come into thermal equilibrium with the reflector, then diffuse as thermal neutrons. Some return to the reactor core to cause another fission. Eventually, some of the neutrons in the reflector-moderator find their way to the beam tube entrance and leave as a neutron beam. The neutron distribution in the moderator is nearly isotropic, so that it makes little difference whether neutron beams stream from the moderator in radial directions from the reactor, or tangentially. The tangential arrangement is favorable because uncollided fast neutrons then have no line-of-sight paths to the outside world, where they cause background radiation problems.

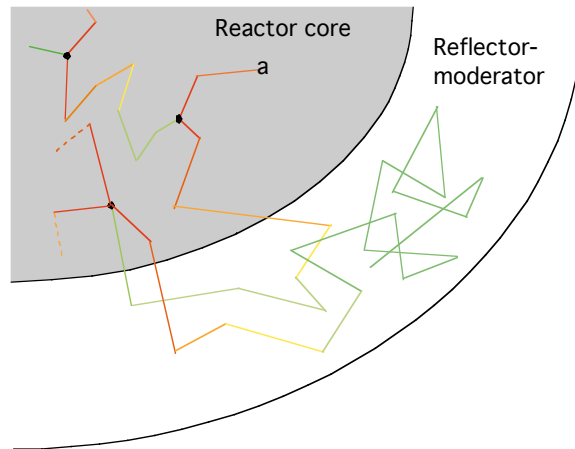


Figure 6. Paths of neutrons in a research reactor. Several fast neutrons (red) emerge from each fission (heavy dots) and proceed to collide, losing energy in each collision (progressively less red) until they cause another fission, disappear by non-fission absorption (a), or travel into the reflector. In the reflector-moderator, neutrons collide repeatedly, losing energy (less red, more green) until they come into thermodynamic equilibrium with the moderator medium (thermal neutrons, green) and live for a long time. Some return to the core to cause another fission. Others find their way into the neutron beams.

Cold Sources

For the purposes of an increasingly large number of scientific applications, it is useful to have a plentiful source of neutrons with lower energies than room temperature implies. Therefore all modern neutron research facilities include at least one *cold-neutron source*, a special moderator maintained at cryogenic temperature, where neutrons can equilibrate to lower average energies. Typically this is a volume of liquid hydrogen, H_2 or D_2 , at a temperature of 20-30 K, imbedded in the main room temperature moderator and providing a number of cold-neutron beams. Fast neutrons and room-temperature thermal neutrons enter the cold moderator where they slow down and *thermalize* at the lower temperature. Liquid D_2 sources contain around ten liters of the liquid. Liquid H_2 sources are typically hollow cavities with a centimeter-or-so-thick shell filled with the liquid. The difference comes about because H_2 is a more effective moderator than D_2 but must be rather thin because H_2 captures cold neutrons at a considerably higher rate than D_2 . Figure 7 illustrates the action of a cavity-type cold-neutron source in a reactor.

Early cold-neutron sources were simple cylinders filled with L- H_2 or L- D_2 (the first was a volume of liquid H_2 that P. A. Egelstaff installed in the BEPO reactor at Harwell, UK, in the 1960s).

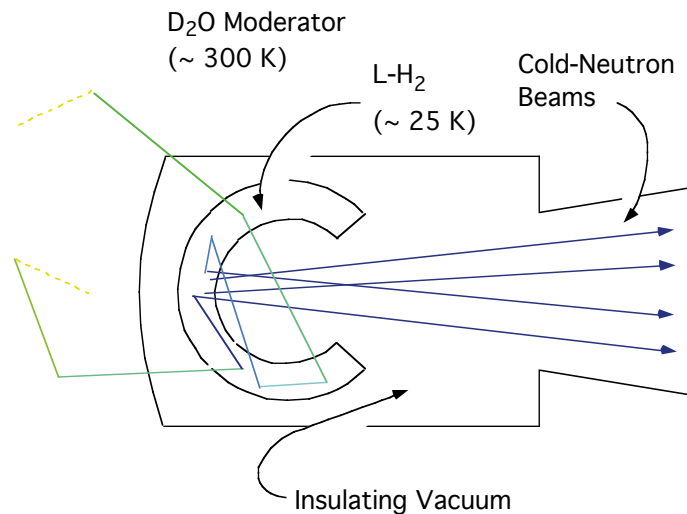


Figure 7. A cavity-type cold moderator. Thermal neutrons (green) enter the 25-K liquid hydrogen from the 300-K D_2O moderator. There, they collide numerous times, losing energy at each collision (less green), and come into equilibrium with the hydrogen at 25 K (blue). The reentrant cavity acts as a hohlraum, allowing neutrons to rattle around within, promoting thermal equilibration but permitting cold neutrons to emerge efficiently into the neutron beams. The diagram exaggerates the thickness of the $L-H_2$ layer in relation to the diameter of the cavity and omits the necessary plumbing arrangements.

Liquid- D_2 cold sources are of comparable design to the cavity type and function in a similar way, but the cold moderator is a somewhat less extreme *hohlraum* with a considerably greater (~ 10 liters) cold $L-D_2$ volume. Neutrons emerge from the moderator in a nearly isotropic distribution. Typically, clusters of *neutron guide tubes*, which view the cold source, carry neutron beams from cold moderators to neutron scattering instruments. We will describe neutron guide tubes in more detail later.

Hot Sources

Just as cold moderators enhance the intensity of available low-energy neutrons, so can hot moderators enhance the intensity of higher-energy neutrons. The High Flux Reactor at the Institute Laue-Langevin includes such a hot source. The moderating medium is graphite, self-heated by fast neutrons and gamma radiation from the reactor to a temperature of about $2000^\circ C$ (2300 K). Thermal neutrons from the surrounding 300-K D_2O moderator enter the hot graphite, about 10 liters in volume, where they collide many times and come into thermodynamic equilibrium with the hot material, as Figure 8 illustrates. Hot, 2300-K, neutrons, average energy about 0.2 eV, emerge into neutron beams and the supported instruments.

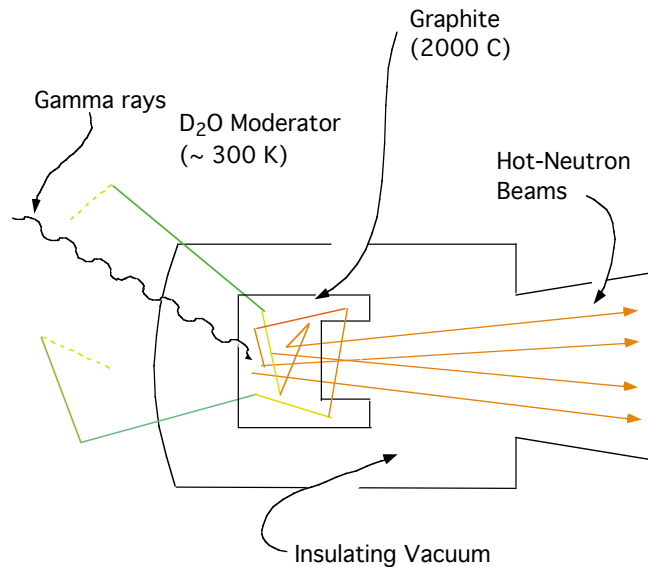


Figure 8. A hot-neutron source. Thermal neutrons (green) from the 300-K D₂O moderator enter the block of vacuum-insulated graphite, heated by gamma rays and fast neutrons to about 2000°C. There they collide, gaining energy in collisions (progressively yellower), and come into thermodynamic equilibrium with the hot graphite. They emerge as hot neutrons (orange) and travel into the neutron beams.

Pulsed Source Moderator/Reflector System

Pulsed source moderators respect dual constraints: The pulses must remain short so as to provide good time resolution; the intensity must be as high as possible within this constraint. In the moderator, initially fast (> 1 MeV) neutrons slow down to useful energies (< 1 eV) and emerge in the direction of the neutron beam (path 2 in Figure 10). The moderator medium is always of material with a high proton density because hydrogen is both light (average energy loss per collision = $1/2$) and has a high neutron scattering cross section. The standard against which alternatives are measured is H₂O, in which the proton density is 6.7×10^{22} protons/cm³. Moderators rest as close as possible to the primary neutron source (the neutron-producing target). Surrounding the moderator is a reflector, typically of Be, which re-directs neutrons that would have missed the moderator, providing them another chance to slow down in the moderator and contribute to the slow neutron beam (path 1 in Figure 10). Path 2 is the normal path, in which neutrons from the source collide and slow down in the moderator then leak out in the direction of the beam. The reflector also returns into the moderator some of the neutrons that leak out before slowing down, for another chance to contribute to the beam (path 4 in Figure 10). Meanwhile, to preserve the short pulses of thermal neutrons in the moderator itself, a layer of “decoupling” material, typically Cd, separates the moderator from the reflector, absorbing neutrons that diffuse for long times as thermal neutrons in the reflector, but passing those of higher energies (> 0.5

eV), which live for much shorter times in the reflector. A “void liner,” also typically of Cd, performs the same function in the beam channel (path 5 in figure 10). This concept [12] and modifications of it are common to all modern pulsed neutron beam sources.

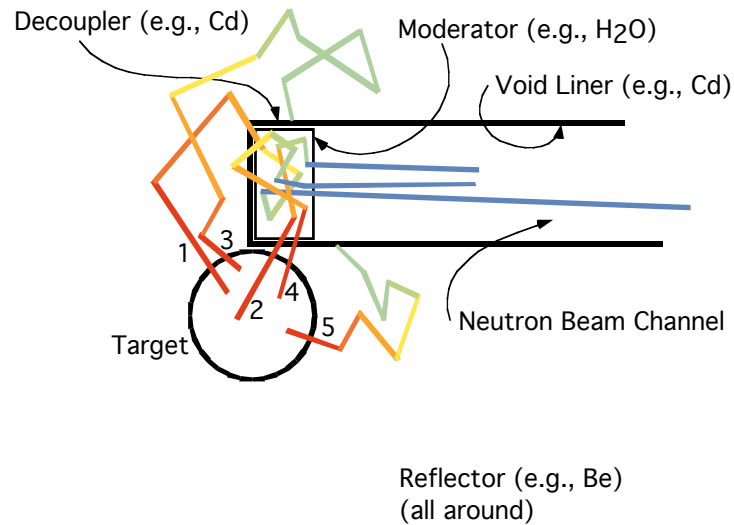


Figure 10. The concept of the decoupled moderator/reflector system. [12]

Source Flux Spectra

The designs of various moderators at steady sources and at pulsed sources proved differently optimized spectra, according to the nature of the source and the intended applications. Steady sources maximize the slow-neutron flux, with moderators of different temperatures and suitable moderator materials. Figure 11 shows the calculated (steady) flux spectra $\phi(\lambda)$ at the source plane of the moderators of FRM-II. [11] The angular distribution of the neutrons is approximately isotropic at the source, that is, uniformly distributed over 4π solid angle at each point. For reference, the reactor power is 20 MW.

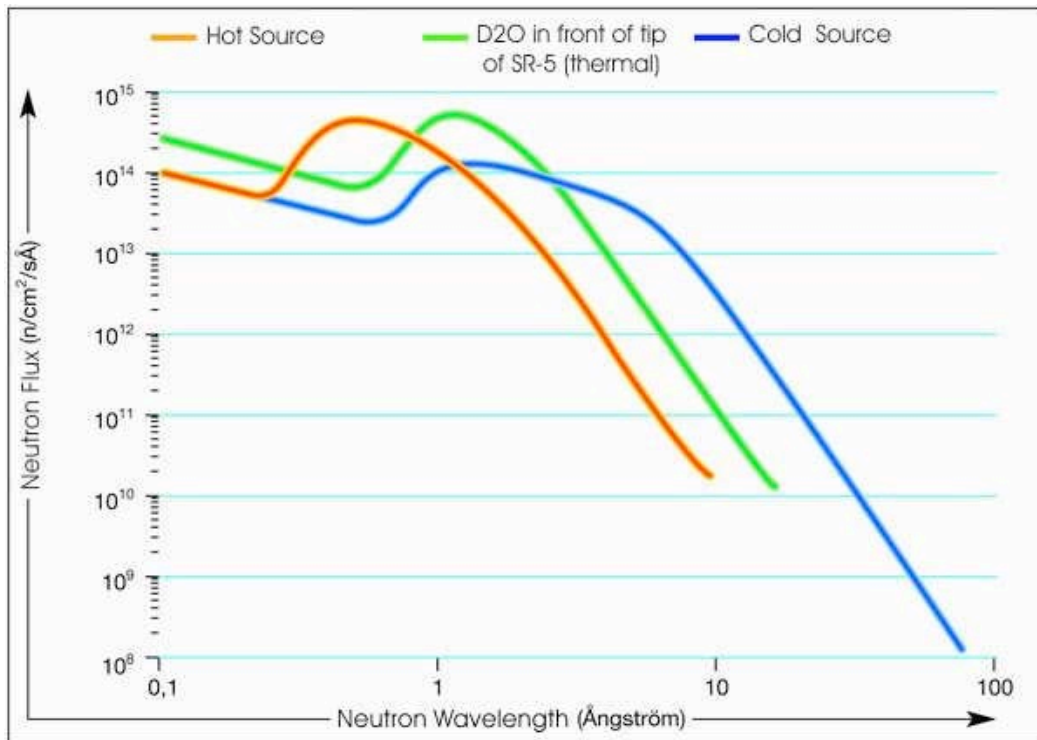


Figure 11. Flux spectra at the source surfaces of the three moderators of the FRM-II reactor.[11]

3. Characterization of Sources

Representation of Source Spectra

Most moderators exhibit a spectrum with a low-energy component of Maxwellian form (liquid hydrogen is an outstanding example for which this is untrue), which joins smoothly to a high-energy component of “slowing-down” form. Figure 11 represents the spectra as the product of energy times the flux per unit energy, $EI(E)$. A “modified Westcott function” [13, 14] provides a good representation:

$$EI(E) = I_{Th} \frac{E^2}{E_T^2} \exp(-E/E_T) + I_{epi} \left(\frac{E}{E_{Ref}} \right)^\alpha \Delta(E),$$

where the “joining function” is

$$\Delta(E) = 1 / [1 - (E / E_{co})^s].$$

I_{Th} and I_{epi} are the amplitudes of the thermal and slowing-down components. E_T is the mean thermal energy, usually larger than $k_B T$, in which T is the physical temperature of the moderator medium. Because the Maxwellian term is small at 1. eV, customarily $E_{Ref} = 1.0$ eV, so that $EI(E)_{1.0 \text{ eV}} = I_{epi}$. Choice of E_{Ref} is arbitrary, at the user’s discretion. The exponent α is called the “leakage exponent” (introduction of this nonleakage factor is the modification of the original Westcott function) because it comes about as a consequence of the slowing-down leakage probability of moderators. E_{co} is a “cutoff energy;” usually $E_{co} \approx 5. E_T$. The “cutoff exponent” s governs the sharpness of the descent of the slowing-down component at low energies. Representative values of these parameters differ considerably between reactor moderators and pulsed-source moderators.

In reactors, the spectral temperature is rather near to the physical temperature and the ratio I_{Th} / I_{epi} is typically of the order of 100. The cutoff exponent s is ~ 7 . Because reactor moderators by design store thermal neutrons for long times, the moderators are large and the leakage exponent is near 0. The angular distribution of neutrons from reactor moderators is approximately isotropic (distributed over 4π solid angle) and constant in terms of position on the viewed surface at the source end of the beam tube.

Figure 12 shows the spectrum from an ambient-temperature polyethylene, $(CH_2)_n$, moderator operated in the early years of IPNS.

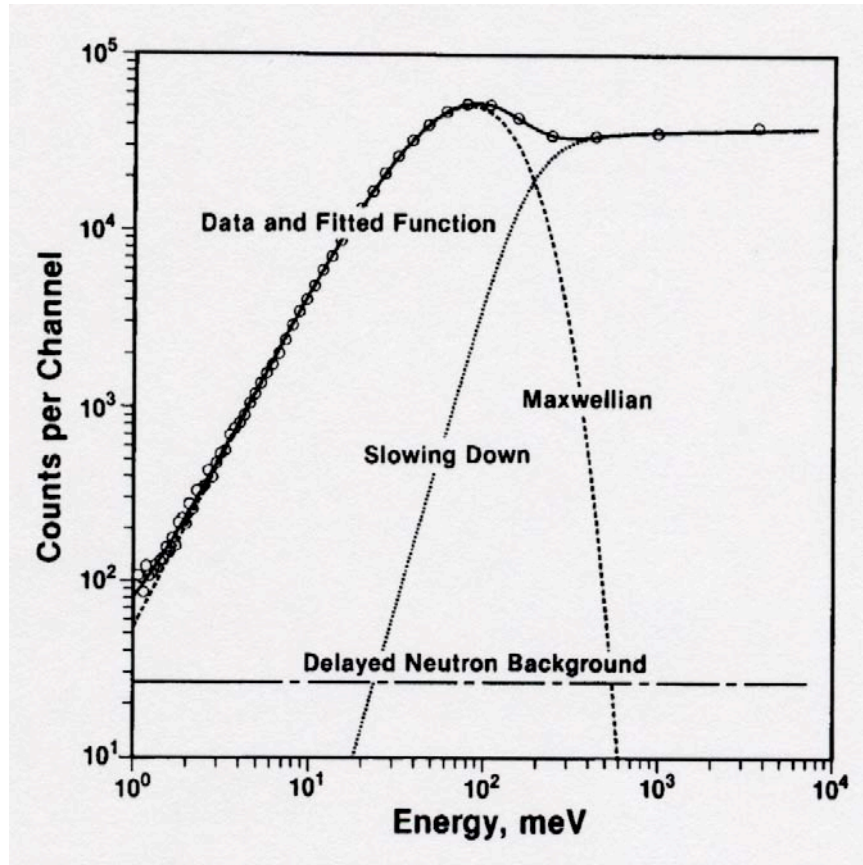


Figure 12. Spectrum of a poisoned room-temperature polyethylene moderator at IPNS [14].

For practical pulsed-source moderators, $1.0 < I_{Th}/I_{epi} < 5.0$ ($I_{Th}/I_{epi} = 2.6$ in the example of Fig. 12, and $E_T = 41$ meV). A typical value for the cutoff exponent for a pulsed-source moderator is $s \sim 3$ to 5 . (In the example, $E_{co} = 180$ meV and $s = 3.5$.) Because of the high leakage probability of pulsed-source moderators, which are small, a typical value is $\alpha \sim 0.05$ (in the example, $\alpha = 0.02$). Nonlinear least-squares codes with fitting parameters starting near these values efficiently fit data from measurements and calculations of steady and pulsed-source moderators except for those of liquid hydrogen.

(Aside: Liquid hydrogen is a famous exception to the rule above because the scattering cross section of para- H_2 , which predominates in the equilibrium state at the temperature of liquid hydrogen, is anomalously small for energies below about 15 meV.)

Pulsed-source moderators have an extra degree of variability compared to the reactor counterparts, in that they can be designed to produce sharp pulses at the sacrifice of spectral intensity. This involves placing a sheet of low-energy threshold absorber (e.g., cadmium) inside the moderator, at chosen depth and parallel to the viewed surface, causing the moderator to look larger or smaller (less or more leaky) to the neutrons within.

Here note that the angular current-density distribution of neutrons at the surface of decoupled pulsed-source moderators is anisotropic, having approximately a Lambert's law dependence on the angle, $\psi(\xi) \sim \cos(\xi)$, where ξ is the angle between the normal and the neutron direction, and is zero for $\xi > 90^\circ$ (that is, neutrons emerge over only the outward-directed 2π of solid angle). Moreover, the spatial distribution of the flux is not flat, but rather in both dimensions perpendicular to the surface, and has an "extrapolated cosine" distribution, $\phi(x) \sim \cos(\pi x/(a+2\delta))$, in which x is measured from the center, a is the width of the moderator surface, and δ is an "extrapolation length" of the order of 1. cm. To a fairly good approximation in the range of angles and positions of interest, the shape of the spectral intensity is independent of angle and position.

The flux of neutrons at a point distant from the source—for example at the sample or beam monitor detector position in a neutron beam, a distance L from the source—is related to the integral over the source area A of the angular current density in the direction of the neutron beam. (At the distant point, the neutron distribution is nearly unidirectional, but the concept of flux is still valid.) Usually the beam direction is nearly perpendicular to the source surface, so that the integrated source intensity is $A\psi(\xi = 0)$ and varies as $1/L^2$ as a function of the distance (the source is so small that it looks like a point from a long distance). It is conventional to characterize the source intensity of steady sources in terms of the 4π -integrated angular current density, that is, the flux Φ_s as measured by an activation foil, so that in the steady-source case, the flux at L is $\Phi_L = \Phi_s / 4\pi L^2$. In pulsed-source moderators the angle-integrated source flux is not a useful quantity, rather, because the angular distribution is biased in the forward direction (Lambert's law), it is the time-averaged, normally emerging angular current per unit solid angle, integrated over the source area, I_s . Then the time-averaged flux at the sample position is $\Phi_L = I_s / L^2$. It is conventional to report calculations and measurements for reactors in terms of the 4π flux at the source, Φ_s ; for pulsed sources, the convention is to report the intensity I_s . All of the previous statements apply for wavelength-specific fluxes $\Phi_s(\lambda)$, $\Phi_L(\lambda)$, $I_s(\lambda)$, etc.

Pulse Shapes of Pulsed-Source Moderators

There is no question of the time-dependence of the neutrons emitted from a reactor (or any steady-source) moderator. However, the time dependence of the neutrons emitted from pulsed-source moderators is of crucial importance, inasmuch as this determines the resolution of time-of-flight measurements. Consequently, the design and optimization of pulsed-source moderators relates closely to the requirements of instruments using the neutrons. Neutrons, initially a very short pulse of high energy, spend time slowing down in the moderator and diffusing around within before emerging. Neutrons emerge in a time distribution that begins at the time of the primary source pulse, as demanded by causality requirements. Figure 13 shows the emission-time distribution of 0.063-eV neutrons from the same moderator as that of Fig. 12. Times t correspond to the times that neutrons cross the moderator surface in the direction of travel and

are measured from the time of the primary source pulse.

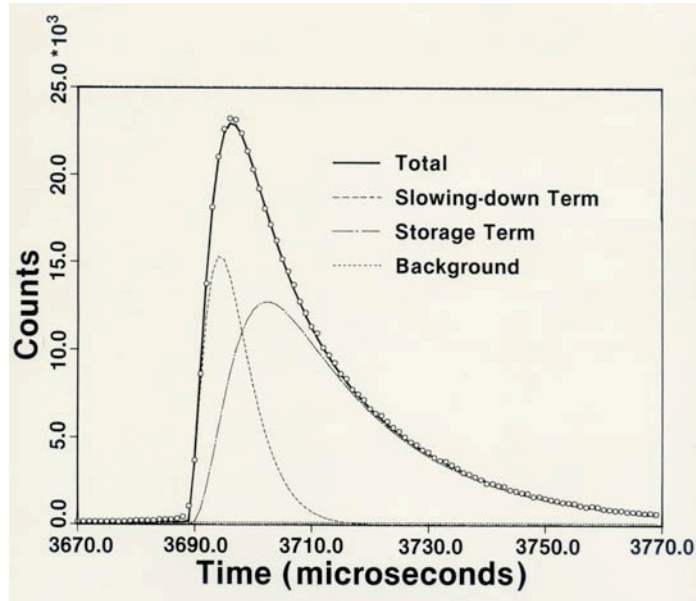


Figure 13. The emission-time distribution of 63.3-meV neutrons of a poisoned room-temperature polyethylene moderator at IPNS. [14,15]

These shapes depend greatly on the wavelength (energy) of the neutrons as well as the details of the moderator. Predominant features of all are the very sharp rising edge and the exponential fall-off at long times. The figure shows a function fitted to the time distribution, which gives an excellent description of the measurement. The function, physics-motivated but basically empirical and called the “Ikeda-Carpenter (I-C) function,” [14,15] is

$$f(E,t) = (1 - R(E))f_{SD}(E,t) + R(E) \int_0^t f_{SD}(E,t') \exp(-b(t-t')) dt'$$

which is the sum of a “slowing-down” function $f_{SD}(E, t) = (st)^2 \exp(-st)$ with $s = v\Sigma(E)$, where $\Sigma(E)$ is the macroscopic scattering cross section for neutrons of energy E , weighted by a factor $(1-R(E))$, and of the same function convoluted with a decaying exponential, $\exp(-\beta t)$, weighted $R(E)$, a “storage” term, which represents the decay of the longest-lived eigenfunction of the moderator neutron distribution. Explicitly, the function is

$$f(E,t) = \left(\frac{s}{2}\right) \left\{ (1 - R)(st)^2 \exp(-st) + \right. \\ \left. + 2R \frac{s^2 \beta}{(s - \beta)^3} [\exp(-\beta t) - \exp(-st)(1 + (s - \beta)t + (s - \beta)^2 t^2)] \right\} .$$

This appears complicated but is not, when viewed in terms of its basis. The function is entirely tractable as a form for least-squares fitting and for subsequent calculation. The parameters s , R ,

and β depend on the energy E ; in concept, β is independent of E , but in terms of the empirical process of fitting, can be taken as E -dependent. The time t for each peak fitted (as in Figure 15 below) must be interpreted as $t_{\text{obs}} - t_0$, in which t_0 is also a fitting parameter. Smooth, even physically reasonable, functions can represent the energy variation of these parameters. This enables representing the functions $f(E, t)$ over the entire range of E in terms of only a few fitting constants. Although devised to fit one particular measurement, the I-C function has been found, sometimes with elaboration, to fit well the emission-time distributions of a wide variety of moderators.

The function $f(E, t)$ does not represent the variation of $I(E, t)$ as an energy density because it is normalized to an arbitrary area both in theory ($\int f(E, t) dt = 1.0$ above) and in measurements.

In time-of-flight applications, the time of arrival at a detector represents the speed (energy, wavelength) of the detected neutron

$$\bar{t} = L/v + \bar{t}_e .$$

This time represents the time measured from the mean time of the emission-time distribution, t_e , which for the I-C function is

$$\bar{t}_e = 3 / (vS(E)) + R(E)/b .$$

Measurements: Spectra

Measuring the energy distribution of the emerging neutrons is straightforward. The object is to determine the time-integrated number of neutrons per unit energy,

$$I(E) = \int_0^{\infty} I(E, t) dt .$$

A detector at a distance L (~ 10 m) from the moderator counts neutrons. It is usually placed in the beam emerging perpendicularly from the viewed surface (this is not usually important because these are usually low-resolution measurements):

$$t = L/v \text{ and}$$

$$C(t) = \eta(v)I(E) \Delta\Omega |dE/dt|.$$

$C(t)$ is the counting rate at time t . $\eta(v)$ is the detector efficiency for neutrons of speed v , (usually a very low-efficiency detector is necessary, for which $\eta(v) = k/v$, where k is a calibration constant). The solid angle subtended by the detector at distance L from the moderator $\Delta\Omega$ is, $\Delta\Omega = A_{\text{det}}/L^2$. Because $E = (m/2)(L/t)^2$, the Jacobian, dE/dt , is $|dE/dt| = 2E/t$. The diagram shows a typical arrangement.

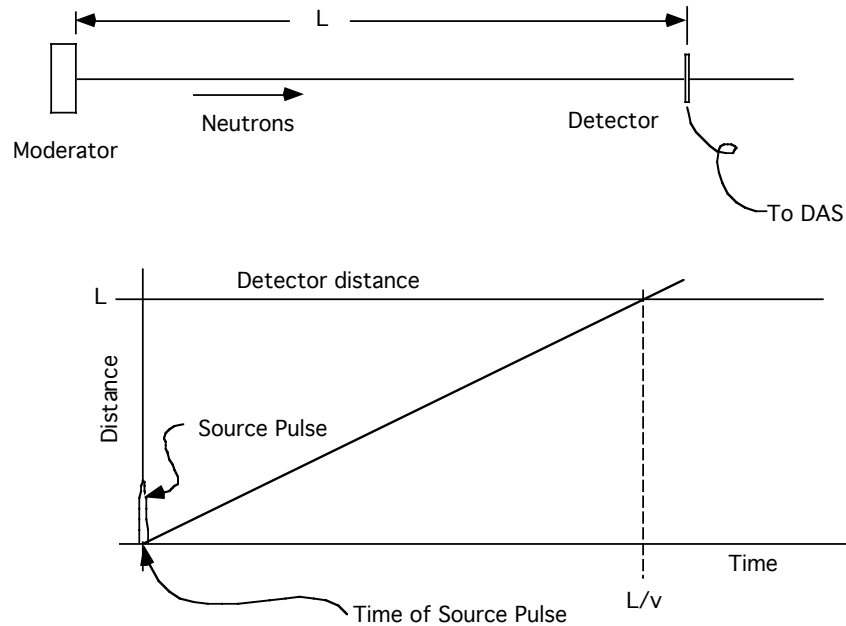


Figure 13. Schematic illustration of an arrangement for measuring the spectrum of neutrons from a pulsed-source moderator. The “time schedule” illustrates the progress of a neutron of speed v .

Measurements of the spectrum from a steady source are probably most simply carried out using the time-of-flight method with a chopper in the beam. Then an additional factor appears in the expression for the counting rate, $T(E)$, the chopper transmission efficiency. And the entire detector must view the entire moderator surface through the chopper aperture.

It is important in practice to acknowledge that materials in the beam between the moderator and the detector attenuate neutrons significantly. Almost inescapable are windows for various purposes and air or other gas, and possibly there are filters and choppers. Air attenuates neutrons in a wavelength-dependent way, about 4% per meter under sea-level conditions, the cross section increasing as the wavelength below about 5 meV energy. Aluminum exhibits numerous Bragg edges (with significant effects of texture), the longest at a wavelength around 4. Å, with the cross section increasing with wavelength at longer wavelengths. The combined attenuation, represented in a factor $F_{\text{att}}(v)$, requires modification of the last result:

$$C(t) \approx \Delta\Omega \int_0^{\infty} F_{\text{att}}(v)\eta(v) I(E, t_e) \left| \frac{dE}{dt} \right| dt_e = \Delta\Omega F_{\text{att}}(v)\eta(v) I(E) \frac{2E}{v} .$$

Measurements: Pulse Shapes

The time distribution of neutrons leaving the moderator is of central importance to the resolution of instruments using neutron beams. The shape of the time distribution $I(E, t)$ varies importantly with E . Measuring $I(E, t)$ requires care to preserve time resolution and to define the energy E that corresponds to each time distribution. The figure illustrates one way to accomplish this with good time-resolution.

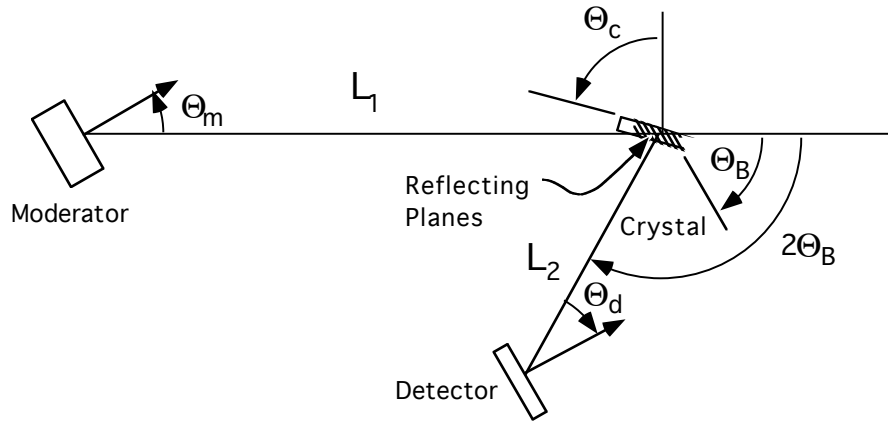


Figure 14. A time-focused crystal analyzer arrangement for measuring emission-time distributions (pulse shapes).

Bragg scattering from a crystal (which can to advantage be a mosaic crystal) reflects neutrons whose wavelengths satisfy the Bragg condition $n\lambda = 2d\sin\Theta_B$ into the detector. Certain “focusing conditions” relating the flight path lengths, the nominal Bragg angle, and the angles of the moderator, crystal physical plane, and the detector plane provide that neutrons that reach the detector do so without significant broadening in time. A Bragg angle $\Theta_B = 60^\circ$ and a moderator viewing angle Θ_m of 18° , with $L_2/L_1 = 0.10$ represents a practical setup. Except for a time delay that separates the different orders, the observed time distributions are faithful replicas of the emission time distribution at each wavelength. Under favorable conditions, up to $n \sim 20$ orders of reflection result from a single setting of the arrangement.

A chopper can provide similar results with greater flexibility in the choice of selected wavelengths, but resolution is relatively poor.

Figure 15 shows a time distribution measured at IPNS by the crystal-analyzer technique. The moderator is poisoned room-temperature polyethylene. The analyzer was Ge(111) cut parallel to the (110) planes, cooled to about 10 K, located 11.7 m from the moderator. The detector was a 3-inch-diameter, 1-mm-thick GS-20 scintillator. Many orders of reflection are visible in the figure, in which the detail is much compressed. Reflections systematically missing among those of the (nnn) diamond lattice show up due to crystal imperfections. Figure 13 above shows the (555) reflection in detail.

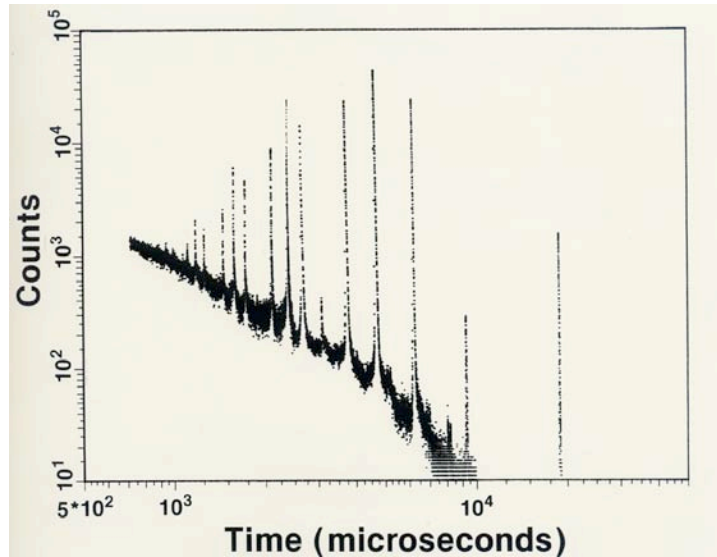


Figure 15. The time distribution of neutrons measured using a time-focused crystal analyzer arrangement.

The time focusing conditions are [15]

$$\tan Q_m = \frac{1}{2} \left(1 + \frac{L_2}{L_1} \right) \cot Q_B,$$

$$\tan Q_d = \frac{1}{2} \left(1 + \frac{L_1}{L_2} \right) \cot Q_B,$$

and

$$\cot Q_c = - \frac{\cos Q_d \tan Q_m + \sin (2Q_B + Q_d)}{2 \sin Q_B \sin (Q_B + Q_d)}.$$

The angles are measured in the same sense as the Bragg angle. Note the implication of an “off-cut” crystal—the physical crystal face is in general not parallel to the reflecting planes. In the instance above, the (111) were the reflecting planes, while the cut face was the (110), differing by 35.3°.

Summary

This section has provided an overview of the methods of producing and moderating neutrons for neutron scattering applications, sketched the means for quantifying spectra and pulse shapes, and indicated how to carry out some of the relevant measurements.

References

- [1] A. M. Weinberg and E. P. Wigner, *The Physical Theory of Neutron Chain Reactors*, The University of Chicago Press (1958). See pages 111-115.
- [2] B. G. Harvey. Chapter 3 “Spallation,” in *Progress in Nuclear Physics*, Editor O. R. Frisch, volume 7, Pergamon Press (1959) see pages 90-120.
- [3] R. Serber, “Nuclear Reactions at High Energies,” *Phys. Rev.* **72**, 11, p 1114-1115 (1947).
- [4] Enrico Fermi, *Nuclear Physics*, Lecture notes from a course given at the University of Chicago, Notes compiled by Jay Orear, A. H. Rosenfeld, and R. A. Schluter, Revised Edition, The University of Chicago Press (1949).
- [5] V. Weisskopf, “Statistics and nuclear Reactions,” *Phys. Rev* **52**, 295 (1937).
- [6] J. S. Fraser, R. E. Green, J. W. Hilborn, J. C. D. Milton, W. A. Gibson, E. E. Gross, and A. Zucker, *Physics in Canada* **21** (2). (1965) page 17.
- [7] J. M. Carpenter, T. A. Gabriel, E. B. Iverson, and D. W. Jerng, “The 10-GeV Question, What is the best energy to drive a pulsed spallation neutron source?” *Physica B* **270**, (1999). Pages 272-279.
- [8] “LWTS, A Long-wavelength Target Station for the SNS,” Argonne National Laboratory report ANL-02/16, Oak Ridge national laboratory Report ORNL/SNS-TM-2001/163. (2002). See section 6.6.
- [9] J. R. Lamarsh, “Introduction to Nuclear Reactor Theory,” Addison Wesley, 1966. See page 168.
- [10] *Ibid*, page 186.
- [11] Forschungsneutronenquelle Garching FRM-II. Secondary Sources.
http://www.frm2.tu-muenchen.de/frm2/secsources/index_en.html
- [12] J. M. Carpenter, “High Intensity, Pulsed Thermal Neutron Source,” U. S. Patent # 3,778,627 (December 11, 1973)
- [13] C. H. Westcott, “Effective Cross Section Values for Well-Moderated Thermal Reactor Spectra,” Chalk River Report CRRP 960 (1959), 3rd Edition Corrected, Atomic Energy of Canada Limited report AECL-1101 (1970).
- [14] J. M. Carpenter and W. B. Yelon, “Neutron Sources,” Chapter 2 in *Methods of Experimental Physics*, editors-in-chief R. Celotta and J. Levine, Volume 23 Part A, *Neutron Scattering*, editors K. Sköld and D. L. Price, Academic Press, Inc. (1986).
- [15] S. Ikeda and J. M. Carpenter, “Wide Energy-Range, High-Resolution Measurements of Neutron Pulse Shapes of Polyethylene Moderators,” *Nucl. Instr. & Methods A*, **239**, 536 (1985).

